Available online at www.sciencedirect.com
SCIENCE DIRECT
International Journal of Thermal Sciences 44 (2005) 53–63
International Journal of Thermal Sciences
www.elsevier.com/locate/ijts

Tree networks for minimal pumping power

Louis Gosselin [a,b,*], Adrian Bejan [a]

[a] *Department of Mechanical Engineering and Materials Science, Box 90300, Duke University, Durham, NC 27708-0300, USA*
[b] *Département de génie mécanique, Université Laval, Québec, Québec G1K 7P4, Canada*

Received 8 February 2004; received in revised form 14 April 2004; accepted 30 June 2004

Available online 12 September 2004

Abstract

In this paper the optimization of fluid networks is based on the minimization of pumping power requirement. The total pipe network volume is constrained. It is shown that only in special cases the minimization of pumping power leads to the same architecture as the minimization of pressure drop or flow resistance. Fundamentals of fluid network optimization are developed for both spanning networks and networks where new non-consumer points are added (Gilbert–Steiner points). It is shown that networks with minimum pumping power must not contain loops. The influence of gravity on the optimization of flow configuration is also addressed. The principles developed in the paper are illustrated with an example representing a set of ten vertices to be connected with pipes. The paper provides designers with more effective basic tools for the conceptual design of fluid networks.

Keywords: Tree networks; Dendritic; Constructal theory; Pumping power; Geometry optimization

1. Introduction

Constructal theory began with the problem of distributing high conductivity material and fast routes (streets) for maximizing the access for heat flow and traffic [1–3]. Dendritic fluid flow structures came next, and were generated based on a deterministic principle—the minimization of global flow resistance, subject to global constraints. The tree-shaped flow architecture emerged as a result, not as an assumption. For this reason the constructal method is unlike the fractal approach, in which the algorithms that generate the geometry are postulated.

The constructal method has been applied to the design of tree networks that transport things other than heat and fluid, for example, electricity, people and goods. This work is reviewed in Ref. [1]. Constructal fluid trees are particularly important because of numerous natural flows that display dendritic architectures, e.g., respiratory air ways, vascularized tissues, lightning, river basins and deltas, and rapid solidification (snowflakes).

In this paper we take a fresh look at the generation of tree architectures for fluid flow, and instead of minimizing the global flow resistance we focus on the minimization of pumping power. It is pumping power, or the minimization of exergy destruction (fuel, food) that governs all the complex flow structures that strive for higher efficiency and persistence (survival) in engineering and nature.

2. The choice of pumping power as a cost function

The very idea of system optimization (in engineering as well as in Nature) implies that the system in question is not purposeless: the system has an objective, a duty to fulfill. This task is accomplished at a certain cost, and under global constraints. Identifying these constraints and objectives is the first conceptual step in the process of designing a system. It is a crucial step that calls for adequate modeling. A flawed cost function may lead to "an optimal" design (optimal in the sense that it minimizes the flawed cost function), but there is

* Corresponding author. Tel.: +1-418-656-7829, fax: +1-418-656-7415.
E-mail address: louis.gosselin@gmc.ulaval.ca (L. Gosselin).

1290-0729/$ – see front matter
doi:10.1016/j.ijthermalsci.2004.06.004

Nomenclature

a	cross-sectional area	m^2
f	friction factor	
g	gravity acceleration	$m \cdot s^{-2}$
I	ratio of pumping power requirement with and without loops	
L	length	m
M	mass conservation equation	
$\dot{m}$	mass flow rate	$kg \cdot s^{-1}$
N	number of vertices	
P	pressure	$N \cdot m^{-2}$
$\dot{s}$	vertex fluid consumption	$kg \cdot s^{-1}$
V	total pipe volume	m^3
$\dot{W}$	pumping power requirement	W
z	altitude	m

Greek symbols

α	parameter characterizing cost per unit length of a pipe	
β	Lagrange multiplier	
ε	exponent to obtain pumping power	
λ	Lagrange multiplier	
ν	kinematic viscosity	$m^2 \cdot s^{-1}$
ρ	density	$kg \cdot m^{-3}$
Γ	path from larger to lower pressures	
$\Omega(\dot{m})$	number of pipes with mass flow rate $\dot{m}$	

Superscript and subscripts

$\sim$	dimensionless parameters
e, k	pipe
i, j	vertex indices

no guarantee that this design provides a satisfactory performance in view of the “real” cost function.

In recent research works on fluid networks (e.g., Refs. [4–7]), pressure drop has been used extensively as a measure of the network operation cost. Optimal networks were generated by minimizing the total pressure drop between the points of highest and lowest pressure. In this section, we argue that this cost function is not always the best choice. In place of pressure drop, pumping power, or destroyed exergy—i.e., in the end what really costs to operate the network—can be used as a more realistic cost function. We show that only in special cases the two cost functions are equivalent leading to the same optimal performance and geometric configuration.

To begin with, consider the simplest situation: a fully developed laminar flow in a pipe with circular cross-section. Given the mass flow rate in the pipe, $\dot{m}$, the pressure drop in the pipe and required pumping power are given by

$$\Delta P = \frac{8\pi \nu \dot{m} L}{a^2} \tag{1}$$

$$\dot{W} = \frac{8\pi \nu \dot{m}^2 L}{\rho a^2} \tag{2}$$

where a and L are respectively the cross-sectional area and length of the pipe. The effect of the pipe geometry (a, L) on the pressure drop and pumping power is the same in this particular case: according to Eqs. (1) and (2), ΔP and $\dot{W}$ are both proportional to (L/a^2).

The situation is different when several pipes are connected together to form a network. In that case, the total pressure drop and pumping power can be written as

$$\Delta P = 8\pi \nu \sum_{e \in \Gamma} \frac{\dot{m}_e L_e}{a_e^2} \tag{3}$$

$$\dot{W} = \frac{8\pi \nu}{\rho} \sum_{e} \frac{\dot{m}_e^2 L_e}{a_e^2} \tag{4}$$

The summation in Eq. (3) is over the pipes e of a path Γ (i.e., over only some of the pipes of the network) from the point of largest pressure to the point of smallest pressure. The summation in Eq. (4) is over all the pipes of the network. It can be shown that the summations in Eqs. (3) and (4) are equivalent if: (i) all the pipes of the network (with a given mass flow rate) have the same length and cross-sectional area; (ii) the quantity $\dot{m} \cdot \Omega(\dot{m})$ is a constant independent of $\dot{m}$, where $\Omega(\dot{m})$ is the number of pipes with a mass flow rate $\dot{m}$.

When conditions (i) and (ii) described above are not respected, pumping power and pressure drop minimization will lead to different network configurations and levels of performance. Therefore, in general, one cannot presume that a minimum pressure drop network will look or perform as a minimum pumping power network.

To illustrate the difference between the two approaches, consider a simple network with one source and two fluid users i and j positioned on a single line, as shown in Fig. 1. The first pipe connects the source with the vertex i, while the second pipe connects i with j. We assume that the points i and j consume the same amount of fluid. Therefore, the mass flow rate in the first pipe is twice as large as in the second pipe. The cross-sectional areas of the two pipes are the parameters to optimize. However, in view of the total pipe volume constraint (see Eq. (7)), there is only one independent variable. We chose the cross-sectional area of the first pipe ($\tilde{a}_1$) as this degree of freedom. According to Eqs. (1) and (2), the total pressure drop and pumping power requirement are:

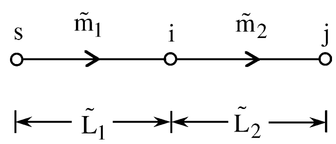

Fig. 1. The discrepancy between pumping power minimization and pressure drop minimization in a simple network with three points.

$$\Delta\widetilde{P} = \frac{\Delta P}{8\pi\nu^2\rho/V^{2/3}} = \frac{\tilde{m}_1\widetilde{L}_1}{\tilde{a}_1^2} + \frac{\tilde{m}_2\widetilde{L}_2}{(1-\tilde{a}_1\widetilde{L}_1)^2} \tag{5}$$

$$\widetilde{W} = \frac{\tilde{m}_1^2\widetilde{L}_1}{\tilde{a}_1^2} + \frac{\tilde{m}_2^2\widetilde{L}_2}{(1-\tilde{a}_1\widetilde{L}_1)^2} \tag{6}$$

where $\tilde{m}_1 = 2$, $\tilde{m}_2 = 1$, $\widetilde{L}_1 = \widetilde{L}_2 = 1$, and the dimensionless parameters are defined later in Section 3. The minimization of the total pressure drop, Eq. (5), leads to the optimal cross-sectional areas $\tilde{a}_{1,\text{opt}} = 0.558$ and $\tilde{a}_{2,\text{opt}} = 0.442$. On the other hand, from the minimization of the pumping power requirement, Eq. (6), it follows that $\tilde{a}_{1,\text{opt}} = 0.614$ and $\tilde{a}_{2,\text{opt}} = 0.386$, which is clearly a different configuration. This conclusion is in accordance with the conditions outlined above for the two approaches to be equivalent. For the network shown in Fig. 1, we have $\Omega_1 \cdot \tilde{m}_1 = 2$ and $\Omega_2 \cdot \tilde{m}_2 = 1$, i.e., that $\Omega(\tilde{m}) \cdot \tilde{m}$ is not a constant.

It also happens that the two approaches, minimum pumping power and minimum pressure drop, are equivalent (i.e., that the above conditions (i) and (ii) are verified) for highly symmetrical geometries. Examples of such a network can be generated when a source located in the center of a circle is connected with fluid users positioned uniformly on the periphery of the circle [6,7]. Other examples are the constructal trees presented in [1]. In general, however, pumping power constitutes a better measure of what it really costs to operate the network. Therefore, in the rest of the paper we rely on pumping power minimization for optimizing fluid networks.

3. Lagrange multiplier method for volume-constrained laminar flow network

Given a set of N vertices (or points), one of which is a source, we want to use pipes to connect the points in order to transport a fluid from the source to the other vertices. For example, the vertices can represent houses in a city, which are to be connected to the city water supply. The method presented in this section can be extended to the problem of connecting a set of points with more than one source. The location of the vertices is known, and so is the consumption—the fluid mass flow rate required at every vortex. It is assumed that the flow in the pipes is laminar and fully developed. The flow regime assumption will be relaxed in Section 5 where it will be shown that the same approach can be used for turbulent flows. The junction losses are neglected.

Two types of constraints are introduced. The first is the total volume of the pipe network,

$$V = \sum_e a_e L_e \tag{7}$$

The second type of constraint is the law of mass conservation at each vertex. The fluid consumption at a given point equals the difference between the inlet and outlet mass flow rates at that point. There are thus N constraints of this type, one for each vertex i,

$$\sum_{j\neq i} \dot{m}_{e(i,j)} = \dot{s}_i \quad \forall i = 1,\ldots,N \tag{8}$$

where $\dot{m}_{e(i,j)}$ is the mass flow rate on the edge (or link) e between vertices i to j. By convection, the mass flow rate is positive when the fluid flows from j to i, and negative when it flows from i to j. The term $\dot{s}_i$ accounts for the fluid consumption of the point i. This can be positive or negative depending on whether the vertex i consumes or produces fluid. If $\dot{s}_i = 0$, then the vertex i neither uses nor delivers fluid. Examples of such points are the Gilbert–Steiner points (GSP) described later in Section 7.

The optimal network is the one that minimizes the cost function (the pumping power, Eq. (4)) subject to constraints (7) and (8). The non-dimensionalized version of these equations is

$$\widetilde{W} = \sum_e \frac{\tilde{m}_e^2\widetilde{L}_e}{\tilde{a}_e^2} \tag{9}$$

$$\widetilde{V} = \sum_e \tilde{a}_e\widetilde{L}_e - 1 = 0 \tag{10}$$

$$\widetilde{M}_i = \sum_{j\neq i} \tilde{m}_{e(i,j)} - \tilde{s}_i = 0 \quad \forall i = 1,\ldots,N \tag{11}$$

where

$$\widetilde{W} = \frac{W}{8\pi\rho\nu^3/V^{1/3}}, \qquad \tilde{m} = \frac{\dot{m}}{\rho\nu V^{1/3}}$$
$$\tilde{s} = \frac{\dot{s}}{\rho\nu V^{1/3}}, \qquad \tilde{a} = \frac{a}{V^{2/3}}, \qquad \widetilde{L} = \frac{L}{V^{1/3}} \tag{12}$$

In summary, the objective is to minimize $\widetilde{W}$ of Eq. (9), subject to $N+1$ constraints, Eqs. (10) and (11). The parameters that can vary are the cross-sectional area of each pipe, and the mass flow rate that each pipe carries. This means two parameters per pipe. Because there are $N(N-1)/2$ possible pipes and the $N+1$ constraints, the number of degrees of freedom (DOFs) to minimize pumping power requirement is $(N^2 - 2N - 1)$. In practical applications, the number of points N is large (e.g., houses in a city), and this yields a high number of degrees of freedom. Even when N is as small as 10, there are 79 DOFs. In general, thus, to obtain an exact solution for this problem is difficult: the use of nested loops is too laborious, while getting stuck in one of the numerous local minima is a danger of the gradient-like method.

The Lagrange multipliers method can be applied to obtain an analogous formulation [8],

$$\frac{\partial\widetilde{W}}{\partial\tilde{a}_k} = \lambda\frac{\partial\widetilde{V}}{\partial\tilde{a}_k} + \sum_{i=1}^{N}\beta_i\frac{\partial\widetilde{M}_i}{\partial\tilde{a}_k} \tag{13}$$

$$\frac{\partial\widetilde{W}}{\partial\tilde{m}_k} = \lambda\frac{\partial\widetilde{V}}{\partial\tilde{m}_k} + \sum_{i=1}^{N}\beta_i\frac{\partial\widetilde{M}_i}{\partial\tilde{m}_k} \tag{14}$$

where λ and β_i are $N+1$ Lagrange multipliers. In view of Eqs. (9)–(11), Eq. (13) becomes

$$\lambda = \frac{-2\tilde{m}_k^2}{\tilde{a}_k^3} \tag{15}$$

The ratio $\tilde{m}/\tilde{a}^{3/2}$ must be a constant for every pipe k. This is true even if the location of the consumers is free to vary, i.e., if parameters $\widetilde{L}_k$ are unknown. Combining Eq. (15) with the cost function (9) we obtain $\widetilde{W} = -\lambda/2$. The Lagrange multiplier λ is thus proportional to the total cost.

Eq. (15) also allows us to rediscover Murray's law, which was used in other network optimization studies where the global objective was the minimization of flow resistance [6,7]. If a stream of mass flow rate $2\tilde{m}$ divides itself in two streams of mass flow rate $\tilde{m}$, then the optimal ratio between the cross-sectional area of the $\tilde{m}$ and the $2\tilde{m}$ pipes is $(\tilde{a}_{\tilde{m}}/\tilde{a}_{2\tilde{m}}) = (\tilde{m}/2\tilde{m})^{2/3} = 2^{-2/3}$, and the optimal ratio of diameters is $2^{-1/3}$.

Similarly, from Eq. (14), we obtain

$$\frac{2\tilde{m}_{k(i,j)}\widetilde{L}_{k(i,j)}}{\tilde{a}_{k(i,j)}^2} = \beta_i - \beta_j \tag{16}$$

where i and j are the two end points of pipe k. When the flow exits from point i on line k, it has to enter by point j, and vice versa. When comparing Eq. (16) with Eq. (1), it is interesting to note that the Lagrange multiplier β_i is proportional to the pressure at vertex i, and that the flow between two points is driven by a pressure difference, ΔP or $\Delta\beta$.

Combining Eqs. (15) and (16), it is possible to express the degrees of freedom as functions of the Lagrange multipliers, and to reintroduce them in constraints (10) and (11),

$$\widetilde{V} = \sum_e \frac{\widetilde{L}_{e(i,j)}^3}{(\beta_i - \beta_j)^2} + \frac{1}{2\lambda} = 0 \tag{17}$$

$$\widetilde{M}_i = \sum_{j\neq i}\left(\frac{\widetilde{L}_{e(i,j)}}{\beta_j - \beta_i}\right)^3 + \frac{\tilde{s}_i}{2\lambda} = 0 \quad \forall i = 1,\ldots,N \tag{18}$$

The optimization problem stated in Eqs. (10) and (11) has been reduced to a set of $(N+1)$ nonlinear equations with $(N+1)$ unknowns—the Lagrange multipliers. Solving Eqs. (9)–(11) is equivalent to solving Eqs. (17) and (18): one can use either approach to obtain the optimal network for a given distribution of points. The first approach has the disadvantage of dealing with many degrees of freedom, while the non-linearity of the equations is an issue in the second approach. In the next sections, we develop another optimization strategy based on Eq. (15).

4. Optimal spanning networks with fully developed laminar flow

So far we have made no assumptions regarding the number of pipes in the network. Furthermore, the formulation presented in the previous section is valid for networks with or without loops. The problem, however, is much simpler in the case of connected topologies with no loops, which are called spanning topologies [9]. Even though this restriction sounds severe, we will see in Section 6 that loops are intrinsically inefficient, and that networks with minimum pumping power cannot contain loops.

For a given set of N vertices, all the spanning topologies have exactly $(N-1)$ pipes. It can be shown that there are N^{N-2} spanning topologies [9]. When a spanning topology is specified, the mass flow rate in each pipe is easy to obtain. It corresponds to the consumption at the vertices connected downstream of the pipe, which is given by the term $\tilde{s}$ in Eq. (9). Because the mass flow rate is known in each pipe, one can take advantage of Eq. (15) by noting that the cross-sectional area of each pipe is also known up to a constant factor—the Lagrange multiplier λ—which is to be determined. Accordingly, the volume constraint (8) can be written as

$$\sum_e \tilde{m}_e^{2/3}\widetilde{L}_e = \left(\frac{-\lambda}{2}\right)^{1/3} \tag{19}$$

As noted in Section 3, there is a proportionality between the Lagrange multiplier λ and the pumping power requirement. The right-hand side of Eq. (19) is the total pumping power raised to the power 1/3, i.e., $\widetilde{W}^{1/3}$. The optimal topology is thus the one that minimizes the left-hand side of Eq. (19). The factor $\tilde{m}_e^{2/3}$ can be seen as the "cost per unit length" of a pipe e. After the optimization, i.e., when the value of the Lagrange multiplier λ is known, the cross-sectional area of each pipe e can be calculated from Eq. (15): $\tilde{a}_e = (-2\tilde{m}_e^2/\lambda)^{1/3}$. Important is that we have reduced the optimization problem of Eqs. (9)–(11) or Eqs. (17), (18) to the search for the optimal topology.

To demonstrate how the present results may be applied, we have chosen a set of 10 vertices distributed non-

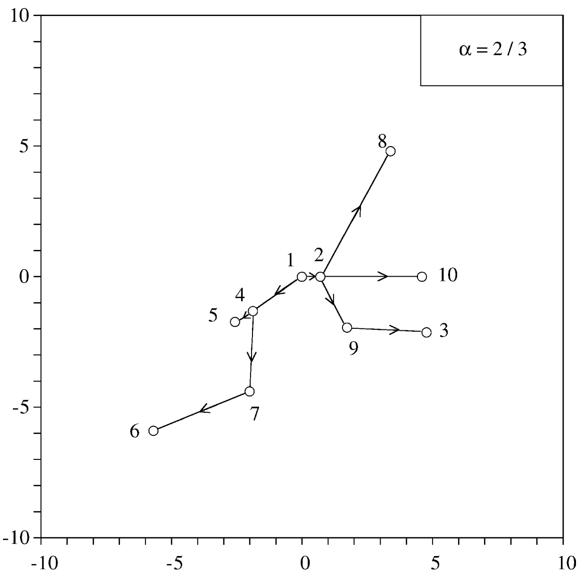

Fig. 2. The minimum pumping power network for a given set of ten vertices, assuming laminar fully developed flow.

Table 1
Relative fluid consumption at each vertex

Vertex i	Fluid consumption, $\tilde{s}_i$	City
1	−1577	Durham
2	276	Raleigh
3	76	Wilmington
4	224	Greensboro
5	186	Winston–Salem
6	69	Asheville
7	541	Charlotte
8	17	Elizabeth City
9	121	Fayetteville
10	67	Jacksonville

Table 2
Relative distance between vertices i and j

i	$j = 10$	9	8	7	6	5	4	3	2
1	4.6	2.6	5.9	4.8	8.2	3.1	2.3	5.2	0.7
2	3.9	2.2	5.5	5.2	87	3.7	2.9	4.6	
3	2.0	3.1	7.0	7.2	11.0	7.3	6.7		
4	6.6	3.6	8.1	3.1	6.1	0.8			
5	7.3	4.2	9.0	2.7	5.3				
6	11.8	8.4	14.2	3.9					
7	7.8	4.5	10.7						
8	5.1	6.9							
9	3.4								

uniformly. These points correspond to 10 cities in the state of North Carolina. The objective is to design a fluid network that connects all the points, provided that one of them is a source of fluid (gas, oil, water, etc.). Vertex 1 was chosen to be the fluid source. To make the problem more realistic, we assume that the consumption of fluid in the city is proportional to the total number of inhabitants. In other words, the term $\tilde{s}_i$ in Eq. (11) is not a constant, but varies with the size of the city considered. Tables 1 and 2 provide the data [10] that have been used. All the spanning topologies ($N^{N-2} = 10^8$) for this specific set of points have been generated numerically. The quantity $\sum_e \tilde{m}_e^{2/3} \widetilde{L}_e$ was then calculated for each topology. The topology shown in Fig. 2 has been found to be the one requiring the smallest pumping power, $\widetilde{W}_{\min} = 5.6335 \times 10^8$. Choosing any other way for connecting the points would result in a larger pumping power requirement.

5. Spanning networks with fully developed turbulent flow

The results presented above for laminar regime can be extended to the turbulent regime. The following empirical relation for the friction factor is commonly used for turbulent fully developed flow in a smooth pipe [11]:

$$f = 0.046\left(\frac{2\dot{m}}{\mu\pi^{1/2}a^{1/2}}\right)^{-1/5} \tag{20}$$

Table 3
Values of α and ε for several flow regimes

Flow regime	α	ε
Fully developed laminar flow	2/3	3
Fully developed turbulent flow in smooth pipes	14/17	17/5
Fully developed turbulent flow in rough pipes	6/7	7/2

Therefore, the dimensionless pumping power required for driving the flow through pipe e is

$$\widetilde{W}_e = 0.0032\frac{\tilde{m}_e^{14/5}\widetilde{L}_e}{\tilde{a}_e^{12/5}} \tag{21}$$

The total pumping power for a network where all the pipes are smooth and carry turbulent flow is the sum of the pumping power required for each pipe, Eq. (21). With the help of Eq. (13), we find a new Lagrange multiplier for this regime,

$$\lambda = \frac{12\tilde{m}_k^{14/5}}{5\tilde{a}_k^{17/5}} \tag{22}$$

It can be shown that the total pumping power requirement $\widetilde{W}$ is still proportional to λ, and that the cost per unit length of pipe with fully developed turbulent flow is $\tilde{m}_e^{14/17}$.

In rough pipes with turbulent flow the friction factor is practically constant and depends on roughness. In this case the pumping power required for pipe e is

$$\widetilde{W}_e \sim \frac{\tilde{m}_e^3\widetilde{L}_e}{\tilde{a}_e^{5/2}} \tag{23}$$

It is easy to show with the Lagrange multiplier method that the cost per unit length of a fully developed turbulent flow in a rough pipe is $\tilde{m}_e^{6/7}$.

In conclusion, one can state the optimization problem more generally as follows: given a set of N points, minimize $\sum_e \tilde{m}_e^\alpha \widetilde{L}_e$, where α changes when the flow regime changes. The exponent α is smaller for laminar flow (2/3) and larger for turbulent flow (6/7 for rough pipes; 14/17 for smooth pipes). In all cases, we have $0 < \alpha < 1$. We will see in Section 6 that the domain occupied by α is why a minimal-power network cannot contain loops. The minimum pumping power requirement is

$$\widetilde{W}_{\min} \propto \left(\sum_e \tilde{m}_e^\alpha \widetilde{L}_e\right)_{\min}^\varepsilon \tag{24}$$

where ε also depends on the flow regime: $\varepsilon = 3$ for laminar flow, 17/3 for turbulent flow in smooth pipes, and 7/2 for turbulent flow in rough pipes. Note that the value of ε does not influence the optimal configuration of the network. The value of ε influences only the relative performance of the network. The values of α and ε for the different flow regimes considered in this paper are summarized in Table 3.

For the sake of illustration, the set of ten vertices used in Section 4 has been used here to construct optimal turbulent flow spanning networks. The same procedure as in Section 4 was used, except that now the value of α is larger: 14/17 for

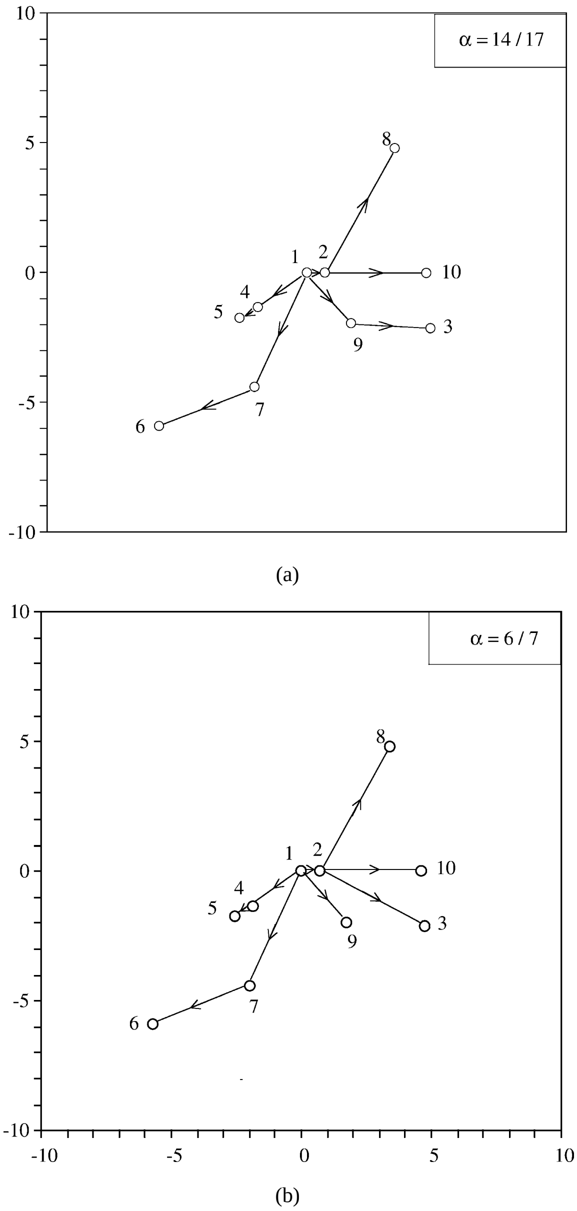

Fig. 3. The minimum pumping power network for a given set of ten vertices, assuming turbulent fully developed flow in smooth (a) and rough (b) pipes.

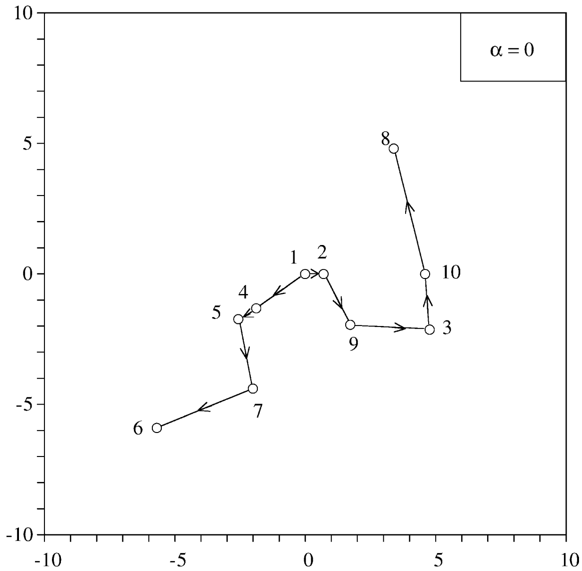

Fig. 4. The shortest network connecting the set of ten vertices.

Table 4
The relative increase in pumping power when a non-optimal network is used

Flow regime	Fig. 4	Fig. 2	Fig. 3(a)	Fig. 3(b)
Laminar ($\alpha = 2/3$)	15.6%	0	6.6%	9.4%
Turbulent, smooth pipes ($\alpha = 14/17$)	36.4%	6.5%	0	0.3%
Turbulent, rough pipes ($\alpha = 6/7$)	44.9%	10.5%	0.2%	0

smooth pipes and 6/7 for rough pipes. The optimal topologies are shown in Fig. 3(a) and (b). Note that the optimal topology depends on the flow regime: the different values of α used in Figs. 2–4 represent different optimal networks.

It is interesting to note in the limit $\alpha \to 0$ the problem reduces to the well-documented minimum spanning tree problem—the search of the shortest tree or the Steiner tree problem if one introduces new non-consuming points (Section 7) [9,12]. The length of one duct that crosses an area element has been used in Ref. [4] as a cost function to minimize. The shortest tree (optimal topology for $\alpha = 0$) for the set of 10 vertices used above is depicted in Fig. 4. This can be done easily with Kruskal algorithm [12]. Furthermore, when $\alpha \to 1$, the problem is trivial and the solution is a network where each point is connected to the source with its own pipe.

Another important aspect is how a network performs when it is optimized for one flow regime and it is used for another regime. This means that the actual value of α is different than the one used to optimize the network. For example, the network depicted in Fig. 2 is optimal for laminar flow ($\alpha = 2/3$), but how does it compare with the networks of Fig. 3 when the flow is turbulent? We want to evaluate to what extent the optimized networks are robust with respect to the flow regime assumption. The pumping power requirements for the networks of Figs. 2–4 have been calculated for different flow regimes. The increase in pumping power relative to the pumping power minimum for that regime is reported in Table 4. As expected, the greater the difference between the actual value α and the one assumed for the optimization, the greater the increase in terms of pumping power. Although the levels of performance are all of the same order of magnitude, using a non-optimal network can require a pumping power increase as large as 44.9%.

6. The intrinsic inefficiency of loops

After the optimal spanning topology is determined, it is possible to search for opportunities to add new pipes to create loops in order to reduce the required pumping power and

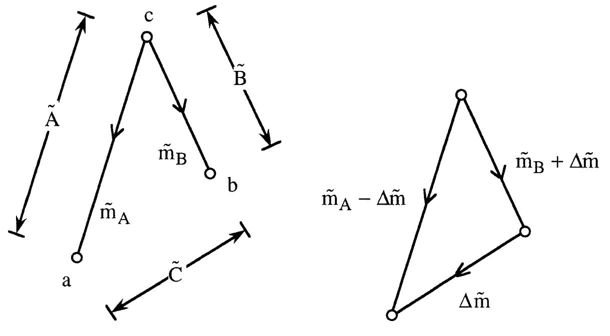

Fig. 5. The addition of a pipe and the creation of a loop.

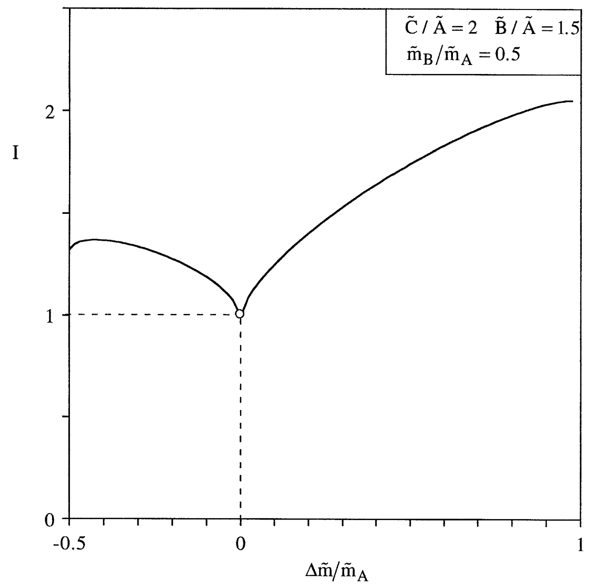

Fig. 6. The function I versus $\Delta\tilde{m}/\tilde{m}_A$, Eq. (27), showing the inefficiency of loops.

to increase robustness. In this section we show that no improvements in global performance can be expected if we follow that path. Consider the triangle presented at Fig. 5. In the absence of a loop, the pipes of length $\widetilde{A}$ and $\widetilde{B}$ carry respectively a mass flow rate of $\tilde{m}_A$ and $\tilde{m}_B$. The total power dissipated in these pipes is

$$\widetilde{W}_{\text{no loop}}^{1/\varepsilon} = \tilde{m}_A^{\alpha}\widetilde{A} + \tilde{m}_B^{\alpha}\widetilde{B} \tag{25}$$

where α is given in Table 3. Next, we form a loop such that the pipe $\widetilde{C}$ carries a mass flow rate of $\Delta\tilde{m}$ from b to a. It follows that the mass flow rates in $\widetilde{A}$ and $\widetilde{B}$ are now given by $(\tilde{m}_A - \Delta\tilde{m})$ and $(\tilde{m}_B + \Delta\tilde{m})$. The total power dissipated in the loop is then

$$\widetilde{W}_{\text{loop}}^{1/\varepsilon} = \tilde{m}_A^{\alpha}\left(1 - \frac{\Delta\tilde{m}}{\tilde{m}_A}\right)^{\alpha}\widetilde{A} + \tilde{m}_B^{\alpha}\left(1 + \frac{\Delta\tilde{m}}{\tilde{m}_B}\right)^{\alpha}\widetilde{B} + (\Delta\tilde{m})^{\alpha}\widetilde{C} \tag{26}$$

The objective is to find whether the $\widetilde{W}$ value of Eq. (26) can be smaller than Eq. (25). The ratio obtained by dividing Eq. (26) by (25) is a function of four parameters $(\Delta\tilde{m}/\tilde{m}_A, \tilde{m}_B/\tilde{m}_A, \widetilde{C}/\widetilde{A}$ and $\widetilde{B}/\widetilde{A})$,

$$I = \left(\frac{\widetilde{W}_{\text{loop}}}{\widetilde{W}_{\text{no loop}}}\right)^{1/\varepsilon} = \left[\left(1 - \frac{\Delta\tilde{m}}{\tilde{m}_A}\right)^{\alpha} + \left(\frac{\tilde{m}_B}{\tilde{m}_A} + \frac{\Delta\tilde{m}}{\tilde{m}_A}\right)^{\alpha}\frac{\widetilde{B}}{\widetilde{A}} + \left(\frac{|\Delta\tilde{m}|}{\tilde{m}_A}\right)^{\alpha}\frac{\widetilde{C}}{\widetilde{A}}\right] \times \left[1 + \frac{\widetilde{B}}{\widetilde{A}}\left(\frac{\tilde{m}_B}{\tilde{m}_A}\right)^{\alpha}\right]^{-1} \tag{27}$$

The parameter $\Delta\tilde{m}/\tilde{m}_A$ is the only one that can be varied freely. This can take values between 1 and $-\tilde{m}_B/\tilde{m}_A$. If the optimal $\Delta\tilde{m}/\tilde{m}_A$ value is 1 or $-\tilde{m}_B/\tilde{m}_A$, the assumption that the initial spanning tree is optimal is not valid, because we would have found another spanning tree with a smaller power requirement. Furthermore, parameter $\widetilde{C}/\widetilde{A}$ must satisfy $|\widetilde{B}/\widetilde{A} - 1| < (\widetilde{C}/\widetilde{A}) < (\widetilde{B}/\widetilde{A} + 1)$, such that abc is a triangle. Note also that the derivative of I with respect to $(\Delta\tilde{m}/\tilde{m}_A)$ is

$$\left.\frac{\mathrm{d}I}{\mathrm{d}(\Delta\tilde{m}/\tilde{m}_A)}\right|_{\frac{\Delta\tilde{m}}{\tilde{m}_A}\to 0_{\pm}} \to \pm\infty$$
$$\left.\frac{\mathrm{d}I}{\mathrm{d}(\Delta\tilde{m}/\tilde{m}_A)}\right|_{\frac{\Delta\tilde{m}}{\tilde{m}_A}\to -\frac{\tilde{m}_B}{\tilde{m}_A}} \to +\infty$$
$$\left.\frac{\mathrm{d}I}{\mathrm{d}(\Delta\tilde{m}/\tilde{m}_A)}\right|_{\frac{\Delta\tilde{m}}{\tilde{m}_A}\to 1} \to \pm\infty \tag{28}$$

where $0 < \alpha < 1$. The function I has three local minima, at $\Delta\tilde{m}/\tilde{m}_A = 1,\ 0$ and $-\tilde{m}_B/\tilde{m}_A$, as illustrated in Fig. 6, where $\tilde{m}_B/\tilde{m}_A = 0.5$. The global minimum is located at $\Delta\tilde{m}_{\text{opt}} = 0$. In conclusion, a fluid network with minimum pumping power cannot contain loops. This basic statement is in agreement with results in the literature where optimal fluid network did not exhibit loops, even when spanning trees were not assumed [5]. This result holds for both laminar and turbulent flows. The presence of loops in a network must be justified by considerations other than minimum pumping power, for example, the need for robustness, to make sure that the network functions if some of the ducts are cut off.

In summary, the optimal fluid network for a given set of vertices is the connected spanning tree that minimizes the quantity $\sum_e \tilde{m}_e^{\alpha}\widetilde{L}_e$. Parameters $\widetilde{L}_e$ and $\tilde{m}_e$ are fully determined when the topology is specified. The cross-sectional area of each pipe can be calculated after the optimization described above. Rather than an infinity of possible solutions, there is thus only a finite number of feasible solutions—the number of feasible topologies, N^{N-2}. This number, however, is quite large.

7. Optimal fluid networks with additional non-consuming points (Gilbert–Steiner points)

So far, we have considered only fluid networks built on the initial set of points, which we identified as spanning trees. The only feasible pipes were the ones that connected two of these initial points. It is well known, however, that one can reduce the cost of a network—in our case the pumping power requirement—by introducing new points that are not fluid consumers. We refer to the 'new' points as Gilbert–Steiner points (GSP) [13]. The location of these additional points can be optimized.

The addition of one GSP in a network adds two more degrees of freedom to the problem: the x and y coordinates of the GSP. It also increases greatly the number of possible topologies, that is the number of ways in which one can connect all the points. Efficient methods of dealing with the addition of GSP are required in order to solve real-life problems involving unsymmetrical systems with large number of points. In this section, we derive some basic properties of the GSP in the fluid networks, and state rules on how to locate them.

The degree of an optimal GSP has to be at least three, which means that a GSP must connect at least three pipes. If only one pipe were connected to a GSP, it would be possible to remove the GSP and its corresponding pipe to reduce the pumping power. If a GSP were in contact with only two pipes, then the GSP can be removed with its corresponding pipes, and a new single pipe can be installed between the points that were previously connected to the GSP to reduce the pumping power. Because of this there is an upper bound for the optimal number of GSPs that one can introduce to reduce the pumping power: this bound is $N - 2$, where N is the number of given points. The properties of the GPSs in a fluid network are very similar to those of the Steiner points [12,14], except that in the optimal fluid network more than three pipes can meet at a GSP.

Only one of the pipes connected to a GSP can bring fluid to the GSP. In other words, there is only one inflow to an optimal GSP. Otherwise, there would be a loop in the network, and we have shown in Section 6 that loops are intrinsically inefficient.

Next, we examine in greater detail the GSP of degree three: one inflow split into two outflows. Even though this is not the most general case, it is by far the most common GSP encountered in both engineering and nature. Consider Fig. 7. The points a, b and c are given, and the mass flows are $\tilde{m}_b$ from a to b, and $\tilde{m}_c$ from a to c. We want to introduce a GSP, named g, in order to reduce the cost function. It can be shown that the optimal angles between the pipes are given by [13,15]

$$\cos(bgc) = \frac{(\tilde{m}_b + \tilde{m}_c)^{2\alpha} - (\tilde{m}_b)^{2\alpha} - (\tilde{m}_c)^{2\alpha}}{2(\tilde{m}_b)^{\alpha}(\tilde{m}_c)^{\alpha}} \tag{29}$$

$$\cos(agb) = \frac{(\tilde{m}_c)^{2\alpha} - (\tilde{m}_b)^{2\alpha} - (\tilde{m}_b + \tilde{m}_c)^{2\alpha}}{2(\tilde{m}_a + \tilde{m}_b)^{\alpha}(\tilde{m}_b)^{\alpha}} \tag{30}$$

$$\cos(agc) = \frac{(\tilde{m}_b)^{2\alpha} - (\tilde{m}_b + \tilde{m}_c)^{2\alpha} - (\tilde{m}_c)^{2\alpha}}{2(\tilde{m}_b + \tilde{m}_c)^{\alpha}(\tilde{m}_c)^{\alpha}} \tag{31}$$

where parameter α is the same as in Section 5, and varies with the flow regime. Important is that for a given topology there is no need for elaborate optimization techniques (looping, gradient method, etc.) to determine the optimal location of a GSP of degree 3: this is delivered in straightforward fashion by Eqs. (29)–(31).

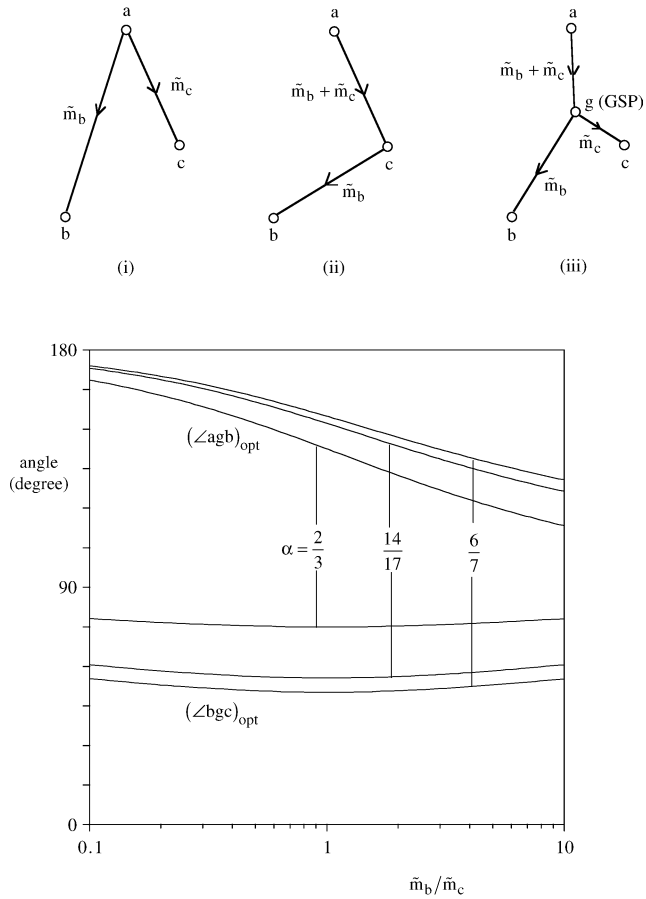

Fig. 7. The optimal angles around a GSP of degree three, Eqs. (29)–(31).

The angles of Eqs. (29)–(31) are reported graphically in Fig. 7. The optimal angle $(bgc)_{opt}$ is almost constant for all ratios $\tilde{m}_b/\tilde{m}_c$, namely $(bgc)_{opt} \sim 75°$ for the laminar regime, 56° for the turbulent regime, smooth pipes, and 50° for the turbulent regime, rough pipes. These results are surprising: the optimal angle made by the two outflowing branches does not vary significantly.

When one of the internal angles of the triangle formed by the vertices a, b, and c is greater than its corresponding optimal angle given by Eqs. (29)–(31) or Fig. 7, no GSP can reduce the cost function. For example, if in the laminar regime the angle bac is larger than 75° (the optimal angle), then one cannot add a GSP to minimize the pumping power requirement. The same conclusion applies to turbulent flow in smooth or rough pipes. This condition can be used to search for opportunities of adding GSPs in a network, simply by looking at the angles formed by the pipes.

The angle condition derived in the preceding paragraphs is only valid for GSP of degree three, but it is a great help when designing a fluid network. For example, when N fluid users are located equidistantly on the perimeter of a disc with a source in the center [4,6], the angle condition can be ap-

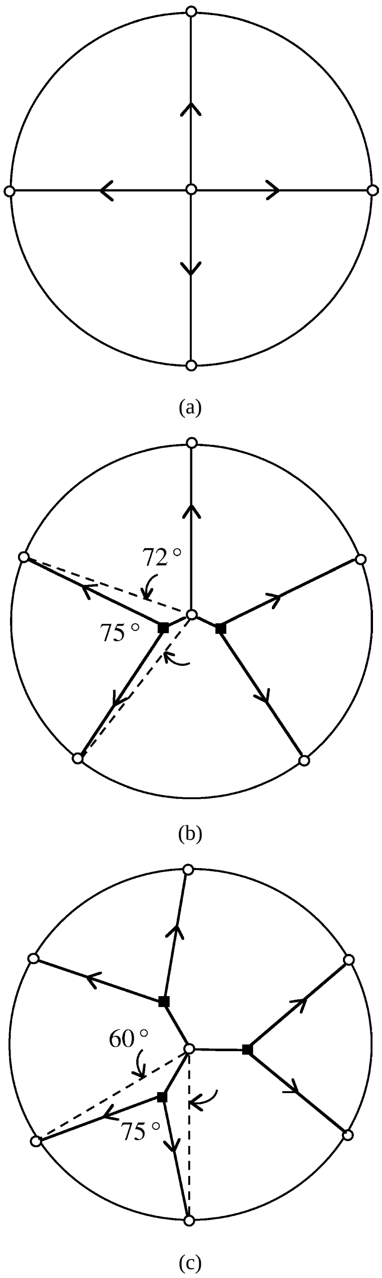

Fig. 8. The addition of GSPs for a simple geometry when the number of vertices increases.

plied to build the optimal network very quickly. Suppose that all the fluid users are connected to the center by means of radial pipes, Fig. 8(a). There is a critical N above which the angle between two pipes becomes smaller than 75° (or 56°, or 50° depending on the flow regime), that is when there is an opportunity for introducing a GSP to reduce the pumping power. As N increases, new opportunities for adding GSPs (or equivalently new levels of branching) arise because the angle between the pipes that issue from the center becomes smaller than 75°. In that case, one can add a GSP of degree three such that the inflow is from the source, and the two outflows go to fluid consumers and make an angle of 75°. This is what is illustrated in Fig. 8. As the number of users increases

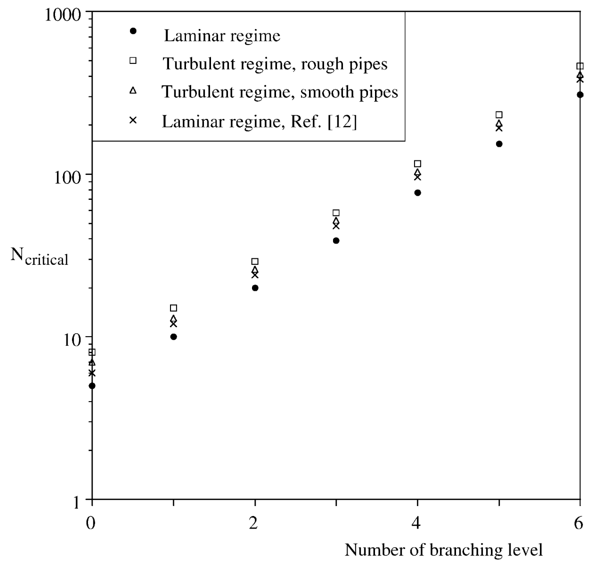

Fig. 9. The critical number of users on the periphery of a circle with a source in the center versus the number of levels of branching.

from 4 to 5, the angle between two radial pipes changes from 90° to 72°. The latter is smaller than 75°, which justifies the introduction of a total of two GSPs such that each GSP generates two outstream branches with the optimal angle of 75°. When $N = 6$, the network is symmetric, and three GSPs can be added, Fig. 8(c). Note that for clarity, the 75° angles in Fig. 8 were drawn larger than 75°.

The optimal network is thus relatively easy to build with the angle condition. We reported on Fig. 9 the optimal number of branching as a function of N for the flow regimes considered in this paper. These results have been deduced simply from the angle condition. Because of symmetry ($\tilde{m}_b/\tilde{m}_c - 1$, Fig. 6), the angle between one outflowing branch and the inlet branch is $(360° - 75°)/2° = 142.5°$. There are no more parameters that can be varied. The results are in good agreements with previous results where the optimal networks for laminar flow were determined by more complicated methods [6]. The difference that remains is due to the fact that in Ref. [6] unsymmetrical trees have not been considered (for example, one level of branching with $N = 5$, Fig. 8(b)). It is worth pointing out, once more, that for these non-symmetrical trees, the minimization of the pressure drop and the minimization of the pumping power will yield different optimal networks, because the conditions described in Section 2 are not respected.

In the example developed in Section 4 for ten cities, there is a maximum of $N - 2 = 8$ GSPs that can be added to reduce the pumping power requirement. To find the optimal network, one would have to investigate all the possible topologies by varying the number of GSPs as well as their degrees. A simpler approach is to reduce the search to GSPs of degree three, such that the location of the GSP is known from Eqs. (29)–(31). Thanks to the angle condition described above, one can focus on triplets (sets of three points), which respect the angle condition. For example, in

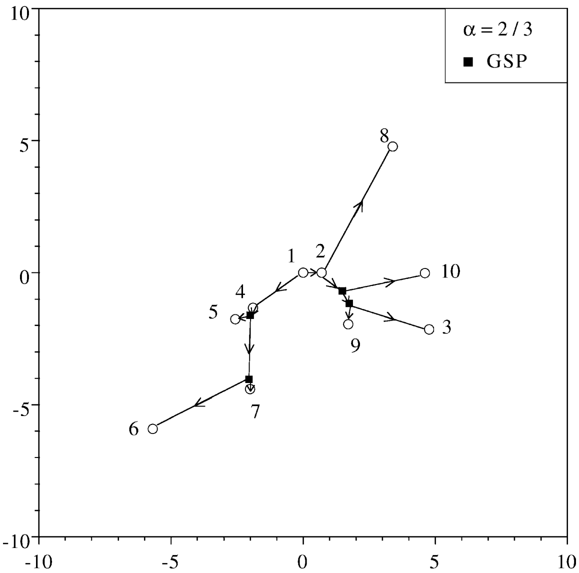

Fig. 10. A nearly optimal network obtained by adding GSPs to the optimal spanning network presented in Fig. 1.

Fig. 2 the two pipes between vertices 2 and 10, and 2 and 9 can be advantageously replaced by three pipes connected with one GSP. We used this approach and added one GSP for every vertex triplet meeting the angle conditions, and we obtained the improved nearly optimal networks presented in Fig. 9. At some point in the optimization, one of the points in the triplets considered is one of the previously added GSPs. This may call for repositioning the oldest GSP so that the angle condition is met. Finally, in Fig. 10 only four opportunities for adding GSPs appeared. The ratio of the pumping power with and without GSPs has been found to be 0.9897. This means that a reduction of the pumping power requirement of approximately 1% is registered when placing the GSPs optimally in that particular network.

8. The effect of gravity on the optimal network

In many networks the initial set of vertices (the fluid users) may not be located in a single plane. The altitude of each point can be different, which will inevitably affect the pumping power requirement because of the gravity forces. An additional term must be included in Eq. (4) to account for gravity. This effect may be detrimental or useful, depending on whether the flow has to overcome gravity or not. We assume in this section that pumping power is needed in each pipe, i.e., that the required flow cannot be generated by gravity alone. We will show that the gravity effect does not change the optimal topology.

We begin by examining the minimum pumping power spanning networks (no GSPs). The total pumping power is given by

$$\widetilde{W} = \sum_{e} \frac{\tilde{m}_e^2 \widetilde{L}_e}{\tilde{a}_e^2} - \tilde{g} \sum_{e(i,j)} (\tilde{z}_i - \tilde{z}_j)\tilde{m}_e \tag{32}$$

where the dimensionless altitude of a vertex is $\tilde{z} = z/V^{1/3}$, and $\tilde{g} = gV/(8\pi\nu^2)$ is a constant. Note that the second summation does not involve the cross-sectional area of the pipes. The Lagrange multipliers method leads to the same expression as in Eq. (15), which allows us to eliminate $\tilde{a}_e$ from Eq. (32),

$$\widetilde{W} = \left(\sum_{e} \tilde{m}_e^{2/3} \widetilde{L}_e\right)^3 - \tilde{g} \sum_{e(i,j)} (\tilde{z}_i - \tilde{z}_j)\tilde{m}_e \tag{33}$$

The second term on the right side of Eq. (33) can be rewritten by changing the summation over all pipes by a summation over all vertices

$$\sum_{e(i,j)} (\tilde{z}_i - \tilde{z}_j)\tilde{m}_e = \sum_{j} \tilde{z}_j \tilde{s}_j \tag{34}$$

where the reference altitude has been set to $\tilde{z} = 0$, at the source. Eq. (34) can be demonstrated as follows. The left side of Eq. (34) does not depend on the distance between points i and j connected by pipe e. Each vertex can be connected to the source with its own pipe without changing the summation, which allows us to write Eq. (34). This rewriting shows explicitly that the gravity effect depends only on the initial set of points.

In conclusion, the new gravity term in Eq. (33) cannot be minimized. This is true regardless of the flow regime. The minimum pumping power for the network may be different with the gravity effect, but the optimal configuration of the network is the same with or without the gravity effect. Therefore, the optimization of the network is still achieved by minimizing the quantity $\sum_e \tilde{m}_e^{\alpha} \widetilde{L}_e$. This conclusion holds even when we consider the addition of GSPs: their contribution to the right-hand side of Eq. (34) vanishes because for GSPs we have $\tilde{s} = 0$.

9. Conclusions

Real-life networks usually involve large number of constituents, for example, houses in a city, cells in a body, or pores in a porous medium. The degrees of freedom that come into play are so numerous that the optimization of such systems is far from being trivial, if at all feasible. Computational limitations may be such that for large numbers of degrees of freedom the time required for optimizing the network exceeds considerably the time available to obtain a solution.

Network designers face time constraints. This observation gives this paper a meaning. By deriving some general and fundamental properties of optimized fluid network, we propose a different approach to this class of problems. The main results presented in this paper may be summarized as follows:

(i) Minimum pumping power networks do not exhibit loops.
(ii) The minimization of network pumping power requirement can be formulated, quite generally, as the search

of the topology that minimizes the quantity $\sum_e \tilde{m}_e^\alpha \widetilde{L}_e$, where α depends on the flow regime, Table 3.
(iii) For a given topology, the optimal location of any GSP of degree three is fully determined by Eqs. (29)–(31). Furthermore, the optimal angle between the two outlet branches of a GSP of degree three is approximately a constant, and depends solely on the flow regime.
(iv) Taking into account the effect of gravity may change the performance of the optimal network, but does not influence the shape of the optimal network, i.e., that it does not change the optimal topology.
(v) Pumping power and pressure drop minimizations are equivalent only in some special cases.

With a set of ten non-uniformly distributed vertices, we illustrated how these fundamental results can be used in practice. However, this paper is intended to be general, and the outcomes apply to any other set of vertices. Another class of problems that could benefit from the present work is when the location of the initial set of points (or alternatively, the parameters $\widetilde{L}_e$) are not known a priori, but are also to be optimized, as in Ref. [1]. Further developments are needed to relax the fully developed flow assumption. A more elaborate model could also take into account the power losses in the junctions.

References

[1] A. Bejan, Shape and Structure, from Engineering to Nature, Cambridge University Press, Cambridge, UK, 2001.

[2] A. Bejan, Constructal-theory network of conducting paths for cooling a heat generating volume, Internat. J. Heat Mass Transfer 40 (1997) 799–816.

[3] A. Bejan, Street network theory of organization in nature, J. Adv. Transportation 30 (7) (1996) 85–107.

[4] S. Lorente, W. Wechsatol, A. Bejan, Tree-shaped flow structures designed by minimizing path lengths, Internat. J. Heat Mass Transfer 45 (2002) 3299–3312.

[5] J.C. Ordóñez, A. Bejan, R.S. Cherry, Designed porous media: Optimally non-uniform flow structures connecting one point with more points, Internat. J. Thermal Sci. 42 (2003) 857–870.

[6] W. Wechsatol, S. Lorente, A. Bejan, Optimal tree-shaped networks for fluid flow in a disc-shaped body, Internat. J. Heat Mass Transfer 45 (2002) 4911–4924.

[7] W. Wechsatol, S. Lorente, A. Bejan, Dendritic heat convection on a disc, Internat. J. Heat Mass Transfer 45 (2003) 4381–4391.

[8] J.E. Marsden, A.J. Tromba, Vector Calculus, fourth ed., Freeman, New York, 1996.

[9] R. Diestel, Graph Theory, second ed., Graduate Text in Mathematics, vol. 173, Springer, New York, 2000.

[10] AAA Georgia, North Carolina and South Carolina Tour Book, 2003 Edition (http://www.aaa.com).

[11] A. Bejan, Convection Heat Transfer, second ed., Wiley, New York, 1995.

[12] F.K. Hwang, D.S. Richards, P. Winter, The Steiner Tree Problem, Annals of Discrete Mathematics, vol. 53, North-Holland, Amsterdam, 1992.

[13] E.N. Gilbert, Minimum cost communication networks, Bell System Tech. J. (1967) 2209–2227.

[14] D. Cieslik, Steiner Minimal Trees, Kluwer Academic, Dordrecht, 1998.

[15] J. Soukop, On minimal cost networks with nonlinear costs, SIAM J. Appl. Math. 29 (4) (1975) 571–581.